tosan 10 in a diameter of 700 nm was sonicated to reduce the particle size to 300 nm. After preparation of NP with different sizes, samples were centrifuged for 1 h at 48,000 rpm for 300-nm NP and at 10,000 rpm for other-sized NP, respectively. After the pellets were freeze-dried overnight, the 40-mg resultant pellets were resuspended in 1 ml of 0.2% (w/v) Tween 80 solution at pH 11.0 to adjust nanoparticle suspension at pH 6.0. For the administration dosage form, 0.01 mg CT and 20 mg OVA were added to 1 ml of resultant NP and incubated at room temperature overnight.

Preparation of CC-Emul

Emulsions with the size of 0.4 μm and 0.7 μm were prepared by a modified ethanol injection method (8). Briefly, 100 mg of soybean oil, 60 mg of EPC, and 60 mg of OA were dissolved in 5 ml hot ethanol, and then 10 ml Milli Q water was added. After ethanol was removed with part of Milli Q water, 5-ml emulsions formed. Then, 0.25 ml of the aqueous solution dissolved with 2 mg Tween 80 and 2 mg chitosan 10 was added to 0.25 ml of the 0.4-μm-size emulsion (total oil and lipid 44 mg/ml) adjusted to about pH 5.0 by 0.1 M NaOH. Chitosan-coated emulsion (CC-Emul, sized 0.4 μm) was prepared by addition of 20 mg of OVA and 0.01 mg of CT to a final volume of 1 ml of the above emulsions with shaking at room temperature overnight. CC-Emul sized 2 μm was prepared as above except using 0.7-μm-size emulsion and double the amounts of each component and addition of Milli Q water slowly by the modified ethanol injection method. This emulsion was diluted 2-fold before use for CC-Emul sized 2 μm.

The cumulant diameter and ζ-potential of the particles in water were measured by the dynamic and electrophoretic light-scattering method, respectively, using a laser light-scattering instrument (Model ELS-800, Otsuka Electronics, Osaka, Japan).

Determination of OVA Adsorption Amount to NP and CC-Emul

The relative adsorption amount of OVA to NP and CC-Emul was calculated by determining the amount of protein remaining in the supernatant after centrifugation at 48,000 rpm, using bicinchonic acid (BCA) protein assay kit (Pierce, Rockford, IL, USA). The adsorption ratio was estimated using the following equation;

$$\text{Adsorption ratio (\%)} = \frac{\text{OVA}_{\text{total conc.}} - \text{OVA}_{\text{supernatant conc.}}}{\text{OVA}_{\text{total conc.}}} \times 100$$

Immunization Protocol and Enzyme-Linked Immunosorbent Assay

Each group of rats was immunized by i.n. and i.p. with one of the following vaccine formulations on days 0, 14, and 28, following the method of Staats *et al.* (9). Fifty microliters of the various-size NP and CC-Emul were administered as approximately 200 g to rats via one nostril with a polyethylene tube. Control rats received the same concentration of OVA and CT in 0.2% (w/v) Tween 80 Milli Q solution.

Blood samples were collected from the jugular vein–anesthetized rats (receiving pentobarbital at a dose of 50 mg/kg following i.p.) via i.p. and i.n. administration on day 35. Sera were separated by centrifugation at 13,000 rpm for 4 min and were stored at 4°C.

Concentrations of IgG and IgA in serum were measured according to the Rat IgG and IgA ELISA Quantitation Kit (Bethyl Laboratories, Montgomery, TX, USA). Titration of rat anti-OVA IgG in serum was measured according to the anti-ovalbumin IgG ELISA Kit (Genesis Diagnostics Ltd, Cambridgeshire, UK).

Statistical Analysis

All values are expressed as means ± SD. Statistical significance of the data was evaluated by Student's *t* test. A p value of 0.05 or less was considered significant. All experiments were repeated at least three times.

RESULTS AND DISCUSSION

Characterization of NP

Considering the toxicity of Tween 80, we prepared NPs by decreasing the concentration of Tween 80. This method showed the size of NP smaller than the method by Lubben *et al.* (7). The characterization of NP is summarized in Table I. The particle size of NP was increased with increasing molecular weights of chitosan. OVA adsorption into NP decreased the ζ-potentials, but remained positive in ζ-potential (about 25 mV) although the adsorbed ratio of OVA was relatively high at greater than 80%. The release of OVA from NP was not observed during 3 h in PBS solution pH 7.2 at 37°C (data not shown).

Particulate vaccine delivery carrier should be targeted to lymphoid tissue as antigen sampling cells provide access to mucosal lymphoid tissue (7). Because the M-cells connecting lymphoid tissue take up antigens and microparticles smaller than 10 μm, particulate systems for antigen drug delivery require micro-size particles to be taken up by M-cells, neither by epithelial cells, nor by drug release upon arrival at the mucosae. Therefore, it was expected that as the particle size of NP obtained in this study was relatively small and the amount of OVA released from NP was low, vaccination may be effectively achieved.

Characterization of CC-Emul

With the addition of chitosan solution at weight ratios greater than 0.1 of chitosan to total oil and lipids in the emulsions, the average diameters of particles became almost con-

Table I. Characterization of NP Without Cholera Toxin

NP (μm)	OVA*	Average diameter (nm)	ζ-potential (mV)	Adsorbed OVA† (%)
0.4	–	310 ± 3.6	27.3 ± 0.5	
	+	385 ± 8.5	24.7 ± 0.6	84.8 ± 0.3
1	–	692 ± 13.6	28.7 ± 0.9	
	+	1102 ± 80	24.7 ± 0.3	89.1 ± 2.0
2	–	1355 ± 168.2	29.3 ± 3.4	
	+	2048 ± 313	25.4 ± 0.6	88.0 ± 1.1
3	–	3080 ± 147.7	32.2 ± 3.9	
	+	3287 ± 419	25.6 ± 0.4	78.9 ± 0.4

NP, chitosan nanoparticles; OVA, ovalbumin. Data are Mean ± SD (n = 3).

* Chitosan nanoparticles (40 mg) adsorbed OVA (20 mg). NP (0.4 and 1 μm), NP (2 μm), and NP (3 μm) were prepared using chitosan 10, 100, and 500, respectively.

† Calculated from the amount of free OVA determined using the BCA protein assay kit.

Table II. Characterization of Chitosan-Coated Emulsion with Ovalbumin (OVA) and Cholera Toxin (CT)*

Emulsions	Average diameter (nm)	ζ-potential (mV)	Adsorbed OVA† (%)
Emulsion (0.4 μm)	362.1 ± 8.4	−48.8 ± 4.1	
Chitosan-coated‡	362.2 ± 13.0	17.0 ± 0.6	
+ OVA and CT§	391.0 ± 6.6	10.2 ± 1.6	96.6 ± 0.2†
Emulsion (2 μm)	729.6 ± 26.6	−48.6 ± 0.9	
Chitosan-coated	897.3 ± 274.1	14.3 ± 2.3	
+ OVA and CT§	1811.3 ± 15.0	10.3 ± 0.8	105.0 ± 11.4†

Data are mean ± SD (n = 3).
* Chitosan-coated emulsion adsorbed OVA and CT (CC-Emul).
† Calculated from the amount of free OVA determined by BCA protein assay kit.
‡ Chitosan 2 mg, total oil and lipid of emulsion 11 mg per ml.
§ OVA 20 mg, CT 0.01 mg per ml of chitosan-coated emulsion.

stant. Corresponding to the change of size, the ζ-potential of negatively charged emulsions became positive by coating chitosan (data not shown). Therefore, for further experiments, the 0.15 weight ratio of chitosan was used to the total oil and lipids of the emulsion for CC-Emul as the chitosan adsorption may be saturated.

After the addition of chitosan to the emulsion, the average diameters of the emulsions increased slightly, while the ζ-potential of the emulsions sized 0.4 μm and 0.7 μm with about −49 mV became 17 mV and 14.3 mV, respectively (Table II). Furthermore, after the addition of OVA and CT, the 362-nm and 897-nm approximate diameters of CC-Emul were increased to 391 nm and 1811 nm, respectively, and their ζ-potential decreased to about 10 mV. The adsorbed ratio of OVA to CC-Emul was nearly 100% (Table II). These results suggested that adequate amounts of chitosan to bind OVA completely existed on the surface of the emulsions. These CC-Emul represent CC-Emul sized 0.4 μm and 2 μm, respectively, from the final size of emulsions. The OVA released from CC-Emul was not detected after 3 h incubation in PBS solution pH 7.2 at 37°C (data not shown). Relatively smaller CC-Emul particles appeared to be more stable than larger ones.

Immunization Following i.p. and i.n. Administration of NP

Figure 1 shows the immune activity of antibody at 35 days after the first immunization following i.p. and i.n. administration of NP. NP following i.p. administration induced significantly higher IgG than control (Fig. 1A). Chitosan has a positive charge and adjuvant activity after i.p. administration in mice (10). Our finding may correspond to the report; the positively charged liposomes are effectively transferred to APC rather than negatively charged ones by i.p. administration (11).

NP following i.n. administration induced significantly higher IgG antibody response compared with control (Figs. 1A and 1B). Production of anti-OVA IgG obtained in this immunization study was comparable to that of IgG in the blood (data not shown). NP sized 0.4 μm and 1 μm showed significantly higher production of IgA compared with the 3-μm-size NP. The uptake of chitosan microparticles has previously been reported (6), but not that of nanoparticles. The reason might be due to the recongnition of NPs by M cells.

Microparticles are retained in the M-cells and induce mucosal immunity, whereas nanoparticles can also be taken up from the NALTs and also induce systemic immunity. Uchida *et al.* reported that 4-μm-size synthetic polymer particles showed higher IgG antibody response than 1.3-μm-size ones for oral administration (12). Jung *et al.* (13) reported that the oral and i.n. administration of the about 0.5-μm-size synthetic polymer particles with negative ζ-potential increased IgG, but those of particles >1 μm did not. However, in the current results, there was no significant difference in the IgG production between the different-size NP following i.n. administration.

Immunization Following i.p. and i.n. Administration of CC-Emul

Although i.p. application of CC-Emul did not increase IgG production compared with control (Fig. 2A), IgA levels

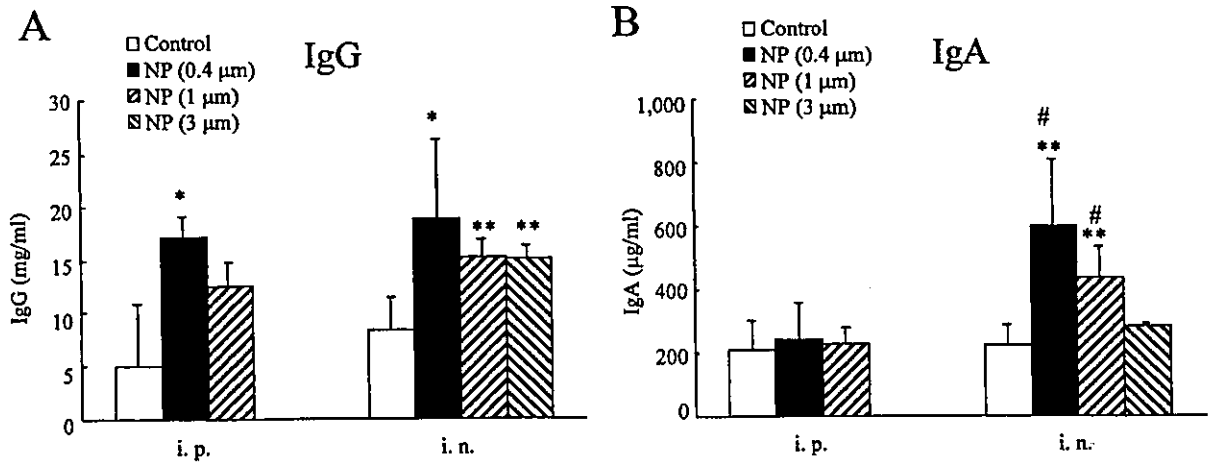

Fig. 1. The (A) IgG and (B) IgA concentrations from rats (n = 3 to 5) immunized by i.p. and i.n. on days 0, 14, and 28 with OVA (5 mg/kg) and CT (2.5 μg/kg) alone for control and NP in Milli Q water. The particle diameter of NP is approximately 0.4 μm, 1 μm, and 3 μm. The sera were collected on day 35. Data are mean ± SD. *$p < 0.05$ and **$p < 0.01$ compared with control, and #$p < 0.05$ compared with NP (3 μm).

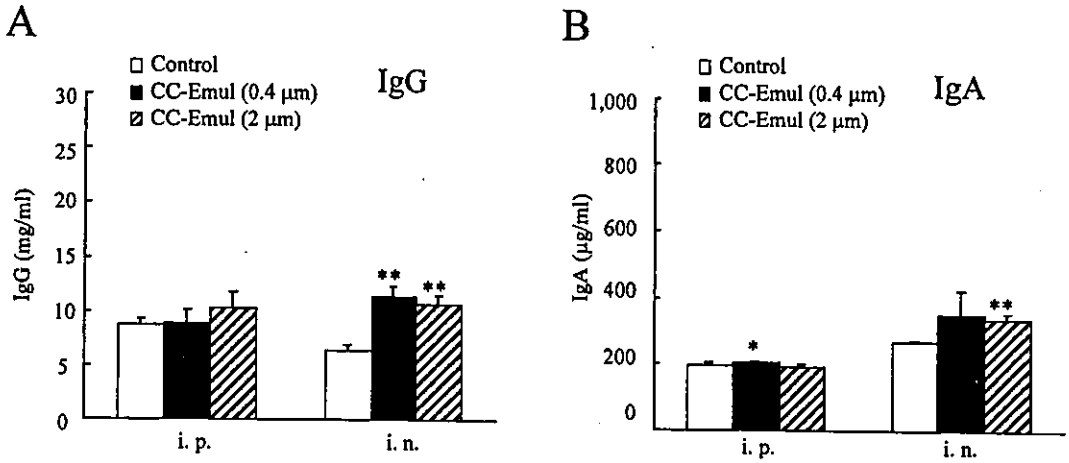

Fig. 2. The (A) IgG and (B) IgA concentrations from rats (n = 3 to 5) immunized by i.p. and i.n. on days 0, 14, and 28 with OVA (5 mg/kg) and CT (2.5 μg/kg) alone for control and CC-Emul in Milli Q water. The particle diameter of CC-Emul is approximately 0.4 μm and 2 μm. The sera were collected on day 35. Data are mean ± SD *$p < 0.05$ and **$p < 0.01$ compared with control.

were similar to those by NP (Fig. 2B). Intranasal administration of CC-Emul sized 2 μm showed significantly higher IgG and IgA antibody responses compared with control. Antibody responses after i.n. administraion between NP and CC-Emul were not different, and each antibody reached similar levels in both particles. No significant difference of IgG and IgA productions was seen between 0.4-μm- and 2-μm-size CC-Emul. This finding corresponds well to NP.

CC-Emul after i.p. administration did not increase IgG production. The reason was not clear, but basically emulsions are easily transferred to lymphoid tissue, so this might render the effect of particle size for immunization by CC-Emul irrelevant. Nevertheless, further experiments are needed to elucidate the difference in the production of antibody by formulations.

CONCLUSIONS

The novel chitosan particles (nanoparticles and emulsions) used simple preparation methods showed high OVA adsorption. OVA was hardly released from each formulation, suggesting that the developed particulate vaccine system may retain antigen on particles until uptake into mucosal membrane. Moreover, chitosan nanoparticles and emulsions administered i.n. induced a significantly higher immune response compared with control, and also, this response was comparable with i.p. injection. From these findings, the chitosan particulate system for nasal vaccine delivery could be a promising candidate.

ACKNOWLEDGMENTS

This project was supported in part by a grant from The Promotion and Mutual Aid Corporation for Private Schools of Japan and by a Grant-in-Aid for Scientific Research from the Ministry of Education, Culture, Sports, Science, and Technology of Japan. We are grateful to Dr. K. Nakamura for his fruitful discussion and to Mr. K. Noguchi and Ms. M. Itabashi for their technical assistance.

REFERENCES

1. M. R. Neutra, E. Pringault, and J. P. Kraehenbuhl. Antigen sampling across epithelial barriers and induction of mucosal immune responses. *Annu. Rev. Immunol.* **14**:275–300 (1996).
2. A. J. Almeida and H. O. Alpar. Nasal delivery of vaccines. *J. Drug Target.* **3**:455–467 (1996).
3. A. de Haan, H. J. Geerligs, J. P. Huchshorn, G. J. van Scharrenburg, and A. M. Palache, and J. Wilschut. Mucosal immuneadjuvant activity of liposomes: induction of systemic IgG and secretory IgA antibody responses in mice by intranasal immunization with an influenza subunit vaccine and coadministered liposomes. *Vaccine* **13**:155–162 (1995).
4. R. J. Soane, M. Frier, A. C. Perkins, N. S. Jones, S. S. Davis, and L. Illum. Evaluation of the clearance characteristics of bioadhesive systems in humans. *Int. J. Pharm.* **178**:55–65 (1999).
5. I. M. van der Lubben, J. C. Verhoef, G. Borchard, and H. E. Junginger. Chitosan for mucosal vaccination. *Adv. Drug Deliv. Rev.* **52**:139–144 (2001).
6. I. M. van der Lubben, J. C. Verhoef, G. Borchard, and H. E. Junginger. Chitosan and its derivatives in mucosal drug and vaccine delivery. *Eur. J. Pharm. Sci.* **14**:201–207 (2001).
7. I. M. Van Der Lubben, F. A. Konings, G. Borchard, J. C. Verhoef, and H. E. Junginger. In vivo uptake of chitosan microparticles by murine Peyer's patches: visualization studies using confocal laser scanning microscopy and immunohistochemistry. *J. Drug Target.* **9**:39–47 (2001).
8. Y. Maitani, H. Soeda, J. Wang, and K. Takayama. Modified ethanol injection method for liposome containing β-sitosterol β-D-glucoside. *J. Liposome Res.* **11**:115–125 (2001).
9. H. F. Staats and F. A. Ennis. IL-1 is an effective adjuvant for mucosal and systemic immune responses when coadministered with protein immunogens. *J. Immunol.* **162**:6141–6147 (1999).
10. K. Nishimura, S. Nishimura, N. Nishi, F. Numata, Y. Tone, S. Tokura, and I. Azuma. Adjuvant activity of chitin derivatives in mice and guinea-pigs. *Vaccine* **3**:379–384 (1985).
11. T. Nakanishi, J. Kunisawa, A. Hayashi, Y. Tutumi, T. Hayakawa, and T. Mayumi. Enhancement of liposome adjuvant actions for tumor vaccines by increasing the degree of positive surface charge. *Drug Delivery System* **13**:151–157 (1998).
12. T. Uchida and S. Goto. Oral delivery of poly(lactide-co-glycolide) microspheres containing ovalbumin as vaccine formulation: particle size study. *Biol. Pharm. Bull.* **17**:1272–1276 (1994).
13. T. Jung, W. Kamm, A. Breitenbach, K. D. Hungerer, E. Hundt, and T. Kissel. Tetanus toxoid loaded nanoparticles from sulfobutylated poly(vinylalcohol)-graft-poly(lactide-co-glycolide): evaluation of antibody response after oral and nasal application in mice. *Pharm. Res.* **18**:352–360 (2001).

Available online at www.sciencedirect.com
SCIENCE DIRECT®
Journal of Controlled Release 97 (2004) 173–183
journal of controlled release
www.elsevier.com/locate/jconrel

Enhanced in vitro DNA transfection efficiency by novel folate-linked nanoparticles in human prostate cancer and oral cancer

Yoshiyuki Hattori*, Yoshie Maitani

Institute of Medicinal Chemistry, Hoshi University, Ebara 2-4-41, Shinagawa, Tokyo, 142-8501, Japan

Received 2 September 2003; accepted 6 March 2004

Available online 17 April 2004

Abstract

Novel folate-linked, cationic nanoparticles (NPs) were developed and evaluated for potential use for gene delivery to human oral cancer (KB cells) and human prostate cancer (LNCaP cells), which abundantly expressed folate binding proteins. Folate-polyethylenglycol-distearoylphosphatidylethanolamine conjugate (f-PEG-DSPE) was incorporated in NPs composed of 3([*N*-(*N'*,*N'*-dimethylaminoethane)-carbamoyl] cholesterol (DC-Chol) and Tween 80. NP-0.3FT, -1FT and -1FLT, which contain 0.3 and 1 mol% f-PEG_{2000}-DSPE, and 1 mol% f-PEG_{5000}-DSPE, respectively, showed about 100–200 nm in size. The NP/plasmid DNA complex (nanoplex) remained in an injectable size (230–340 nm) and slightly increased its size in serum. The association of NP-1FT with KB cells was enhanced by f-PEG_{2000}-DSPE and was blocked by co-incubation with free folic acid in medium. In transfection activity, the NP-1FT, but not NP-1FLT, showed high activity into KB and LNCaP cells in the presence of serum. The NP-0.3FT also showed high activity into LNCaP cells, but not KB cells. In RT-PCR analysis, KB cells strongly expressed folate receptors mRNA, but LNCaP cells did not. In contrast, LNCaP cells expressed mRNA of prostate-specific membrane antigen (PSMA), which interacts with the folate substrate. Uptake mechanism of folate-linked NPs in LNCaP cells may be different from that in KB cells. This is the first report that folate-linked NPs selectively deliver the DNA to LNCaP cells, suggesting that such NPs are potentially targeted vectors to prostate cancer for gene delivery.

Keywords: Cationic nanoparticles; Folic acid; Gene delivery; KB; LNCaP

1. Introduction

Gene therapy has become an increasingly important strategy for treating a variety of human disease, including cancer [1]. The development of suitable delivery vectors for in vivo gene transfer is necessary for the clinical application of therapeutic genes. Synthetic vectors such as a lipid nanoparticle (liposome and emulsion) have become an attractive strategy due to their lack of immunogenicity, the potential for tissue-specific targeting, relative safety and relative ease of large-scale production. The use of cationic liposome/DNA complex (lipoplex) has become one of the most promising methods for in vivo gene delivery [2]. However, cationic liposomes mixed with DNA

* Corresponding author. Tel./fax: +81-3-5498-5048.
E-mail address: yhattori@hoshi.ac.jp (Y. Hattori).

0168-3659/$ - see front matter © 2004 Elsevier B.V. All rights reserved.
doi:10.1016/j.jconrel.2004.03.007

often result in large aggregated lipoplexes [3,4], which cannot be injected in blood vessels and yield very low-level transfection efficiency in vivo [5,6]. Such vectors could be used to achieve an injectable particle size after forming complex with DNA, with resulting high transfection efficiency.

Tissue-targeted gene expression is also an important issue for improvement of safety in gene therapy. A variety of targeting ligands has been examined for targeting liposomes including folate receptors [7–12]. Folate receptor (FR) is known to be abundantly expressed in large fraction of human tumors, but it is only minimally distributed in normal tissues [13–19]. Therefore, the FR serves as an excellent tumor marker as well as a functional tumor-specific receptor.

Folic acid, a high-affinity ligand for FR, retains its receptor-binding and endocytosis properties when covalently linked to a wide variety of molecules. Therefore, the liposomes conjugated to folate ligand via PEG-spacer have been used for the delivery of chemotherapeutic agent to the receptor-bearing tumor cells, e.g. human oral cancer (KB) cells [12]. However, the use of folate ligand as a targeting ligand to deliver DNA has not been successful in in vivo gene therapy [9,10].

Prostate cancer is a significant problem, reported as the leading cancer diagnosed in males [20]. High affinity folate binding protein was characterized in human prostate [21], but the kind of folate binding protein expressed in human prostate has not been reported.

Prostate-specific membrane antigen (PSMA) is a transmembrane protein with an overexpressed pattern specific to human prostate cancer cell line (LNCaP cells) and malignant human prostate tissue [22]. The physiological role of PSMA in prostate cancer remains unknown. It shows hydrolase enzymic activity with a folate substrate [23]. If overexpression of PSMA in prostate cancers represents an advantageous adaptation that allows uptake of folic acid required for rapid division, it could be utilized as a potential target for selective delivery.

In the present study, we prepared folate-linked nanoparticles (NPs) consisting of 3([*N*-(*N'*,*N'*-dimethylaminoethane)-carbamoyl] cholesterol (DC-Chol), Tween 80 and folate-polyethylenglycol-distearoylphosphatidylethanolamine conjugate (f-PEG-DSPE) to form injectable particle-sized complex with DNA (nanoplex) and to maintain the particle size of nanoplexes in serum. Furthermore, we examined the ability of folate linked at the distal end of PEG_{2000}-DSPE to enhance the gene expression in KB and LNCaP cells, and then investigated the uptake mechanism by examining the expression pattern of FRs and PSMA mRNAs in both cells by the RT-PCR method.

2. Materials and methods

2.1. Materials

DC-Chol was purchased from Sigma (St. Louis, MO, USA). Tween 80 (mean M.W.: 1300 Da) and Triton X-100 were obtained from Tokyo Kasei Kogyo (Tokyo, Japan). Folic acid and ninhydrin spray were purchased from Wako (Tokyo, Japan). PEG-lipid (polyethyleneglycol derivative of distearoylphosphatidylethanolamine, PEG-DSPE, mean molecular weight of PEG: 2000 and 5000 Da) was supplied by NOF (Tokyo, Japan). Tfx20, cationic liposome component mixed with L-dioleoylphosphatidylethanolamine (DOPE), was purchased from Promega (Madison, WI, USA). 1,1'-Dioctadecyl-3,3,3',3'-tetramethylindocarbocyanine perchlorate (DiI) was obtained from Lambda Probes and Diagnostics (Graz, Austria). Silica gel 60 F_{254} was purchased from Merck (West Point, PA, USA). The Pica gene luciferase assay kit was purchased from Toyo Ink (Tokyo, Japan). Bicinchonic acid (BCA) protein assay reagent was purchased from Pierce (Rockford, IL, USA). All other chemicals used were of reagent grade. The plasmid DNA (about 6740 bp) encoding the luciferase maker gene under the CMV promoter (pCMV-Luc) was supplied by Dr. Tanaka in Mt. Sinai School of Medicine (NY, USA). All reagents were of analytical grade. Folate-deficient RPMI1640 medium and fetal bovine serum were purchased from Life Technologies (Grand Island, NY, USA).

2.2. Synthesis of f-PEG_{2000}-DSPE and f-PEG_{5000}-DSPE

f-PEG_{2000}-DSPE was synthesized as reported previously [24]. Folic acid was dissolved in dimethyl sulfoxide (1 ml). Amino-PEG_{2000}-DSPE (100 mg,

0.035 mmol) and pyridine (0.5 ml) were added to the folic acid solution followed by dicyclohexylcarbodiimide (32.5 mg). The reaction was continued at room temperature for 4 h. TLC on silica gel 60 F_{254} (75:36:6 chloroform/methanol/water) showed a new spot (R_f=0.57) due to the formation of the product. The disappearance of amino-PEG_{2000}-DSPE (R_f= 0.76) from the reaction mixture was confirmed by ninhydrin spray. Pyridine was removed by rotary evaporation. Water (12.5 ml) was added to the reaction mixture. The solution was centrifuged to remove trace insolubles. The supernatant was dialyzed in Spectra/Por CE (Spectrum, Houston, TX, USA) tubing (MW cutoff of 300,000 Da) against saline (50 mM, two times with 2000 ml) and water (three times with 2000 ml). The dialyzed product was lyophilized and analyzed by ESI-TOFMS mass spectroscopy. Exactly the same protocol was used to prepare f-PEG_{5000}-DSPE from amino-PEG_{5000}-DSPE.

2.3. Plasmid DNA

Protein-free preparation of pAAV-CMV-Luc plasmid was purified following alkaline lysis using maxiprep columns (Qiagen, Hilden, Germany). FITC-labeled plasmid was prepared with Label IT fluorescein labeling kit (Mirus, Madison, WI, USA).

2.4. Preparation of NPs

NP formulae in Table 1 were prepared with lipids (DC-Chol, Tween 80, PEG_{2000}-DSPE, f-PEG_{2000}-DSPE and/or f-PEG_{5000}-DSPE) in 10-ml water by the modified ethanol injection method. In DiI-labeled NPs, DiI was incorporated at 0.04 mol% of the total lipid. Briefly, an appropriate volume of ethanol containing lipids was prepared. The ethanol was removed using an evaporator and finally a semisolid solution was formed. An appropriate volume of water was added to the semisolid solution, and the ethanol contained in the solution was removed by an evaporator. To obtain a uniform particle size distribution, the mixture was sonicated for 5 min in a bath-type sonicator (Honda Electronics, W220R, 200 W, 40 kHz, Tokyo, Japan) and then sterilized by filtration through a sterile syringe-driven filter unit with a pore size of 450 nm at once.

Table 1
Formulae of FR-targeted nanoparticles

Formulation	Mol%				
	DC-Chol	Tween 80 (T)	PEG_{2000}-DSPE (P)	f-PEG_{2000}-DSPE (F)	f-PEG_{5000}-DSPE (FL)
NP-T	95	5	–	–	–
NP-0.3PT	94.7	5	0.3	–	–
NP-1PT	94	5	1	–	–
NP-0.3FT	94.7	5	–	0.3	–
NP-1FT	94	5	–	1	–
NP-1FLT	94	5	–	–	1

Nanoparticles were prepared with lipids [e.g. DC-Chol/Tween 80/f-PEG_{2000}-DSPE=94/5/1, molar ratio=10:1.3:0.65, weight (mg)] in 10-ml water by the modified ethanol injection method.

2.5. Size and ζ-potential of NPs and nanoplexes

The particle size distributions of NPs and nanoplexes were measured by the dynamic light-scattering method, and the ζ-potentials of NPs and nanoplexes were determined by the electrophoresis light-scattering method (ELS-800, Otsuka Electronics, Osaka, Japan) at 25 °C after by diluting of dispersion to an appropriate volume with water. Stability of NPs was assessed by measuring size changes after 60 days. The nanoplex containing plasmid DNA and NPs at the charge ratio (+/−) of 1/1, 3/1 or 5/1 was used to measure the size and ζ-potential. Stability of nanoplex was assessed by measuring size changes after dilutions in 10% or 50% serum.

2.6. Cell culture

KB cells were supplied from Cell Resource Center for Biomedical Research, Tohoku University. LNCaP cells were from the Department of Urology, Keio University Hospital. KB and LNCaP cells were grown in folate-deficient RPMI-1640 medium supplemented with 10% heat-inactivated serum and kanamycin (100 μg/ml) at 37 °C in a 5% CO_2 humidified atmosphere.

2.7. Association of nanoplexes with KB cells

KB cell cultures were prepared by plating KB cells in a 35-mm culture dish 24 h prior to each experiment. Twenty microliters of each DiI-labeled NPs were mixed with 4 μg DNA and then diluted in 1 ml folate-deficient RPMI medium containing 10% serum.

The mixtures were added to the monolayers of KB cells. To determine the selective association of the nanoplex with KB cells, KB cells were incubated with nanoplexes in the presence or absence of 1 mM folic acid. After 1-, 2- and 3-h incubation, the dishes were washed two times with 1 ml PBS (pH 7.4) to remove unbound nanoplex, and the cells were detached with 0.25% trypsin. The cells were centrifuged at 1500 × *g*, and the pellets were lysed with 1 ml of lysis buffer (PBS containing 0.5% Triton X-100). Arbitrary units (a.u.) of DiI fluorescence intensity were then measured using a fluorometer (Hitachi F-4010, Tokyo, Japan) at excitation and emission wavelengths of 550 and 570 nm, respectively. Protein content was estimated using BCA protein assay, and results were expressed as fluorescence (a.u.) per mg/ml of protein lysate.

2.8. Confocal microscopy

KB cells were plated into 35-mm culture dishes. Ten microliters of each NP was mixed with 2 μg DNA and then diluted in 1 ml the complete medium. KB cells were incubated with the mixtures in the presence or absence of 1 mM folic acid for 24 h. After medium removal, cells were washed with PBS and fixed with PBS-buffered 4% formaldehyde solution at room temperature for 1 h, and then washed three times with PBS. Next, the coverslips were put on the dish coated with Aqua Poly/Mount (Polyscience, Warrington, PA, USA) to prevent fading. Examinations were performed with a Radiance 2100 confocal laser scanning microscopy (BioRad, CA, USA). For DiI, maximum excitation was performed by a 543-nm line of internal He–Neon laser, and fluorescence emission was observed with long-pass barrier filter 560DCLP. FITC-labeled DNA was imaged using the 488-nm excitation line of an argon laser, and fluorescence emission was observed with a filter HQ515/30. The contrast level and brightness of the images were adjusted.

2.9. Luciferase assay

The nanoplexes at charge ratios (+/−) of 1/1, 2/1, 3/1, 4/1 or 5/1 of cationic lipid to DNA were formed by addition of NPs to 2 μg DNA with gentle shaking and leaving at room temperature for 10–15 min. For transfection, each nanoplex was diluted in 1 ml complete medium and then incubated for 24 h.

Luciferase expression was measured according to the luciferase assay system. Incubation was terminated by washing the plates three times with cold PBS. Cell lysis solution (Pica gene) was added to the cell monolayers and subjected to one cycle of freezing (−70 °C) and thawing at 37 °C, followed by centrifugation at 15,000 rpm for 5 s. The supernatants were stored at −70 °C until the assays. Aliquots of 20 μl of the supernatants were mixed with 100 μl of luciferase assay system (Pica gene) and counts per second (cps) were measured with a chemoluminometer (Wallac ARVO SX 1420 multilabel counter, Perkin Elmer Life Science, Japan). The protein concentration of the supernatants was determined with BCA reagent using bovine serum albumin as a standard and cps/μg protein was calculated.

2.10. RNA isolation and RT-PCR

Total RNA was isolated from LNCaP and KB cells, respectively, using the NusleoSpin RNA II (Macherey-Nagel, Germany). RNA yield and purity were checked by spectrometric measurement at 260 and 280 nm and RNA electrophoresis, respectively. The first-strand cDNA was synthesized from 5 μg total RNA after denaturation for 5 min at 65 °C by use of 50-pmol random primer, 0.5 mM dNTP and 5 U AMV reverse transcriptase XL (Takara Shuzo, Japan). The reaction was performed at 41 °C for 1 h in a 20-μl volume. For RT-PCR, a 25-μl reaction volume contained the following: 1 μl of synthesized cDNA, 10 pmol of each specific primer pair, 0.25 U Ex Taq DNA polymerase (Takara Shuzo) with a PCR reaction buffer containing 1.5 mM $MgCl_2$ and 0.2 mM of each dNTP. The temperature profile of the PCR amplification consisted of denaturation at 94 °C for 0.5 min, primer annealing temperature at 55 °C for 0.5 min and elongation at 72 °C for 1 min for 30 cycles. PCRs of the housekeeping gene β-actin, FRs (FR-α, -β, -γ) and PSMA were performed at the same cycle run for all samples. The PCR products for FRs, PSMA and β-actin were analyzed by 1.5% agarose gel electrophoresis in Tris–borate–EDTA (TBE) buffer. The products were lighted by ethidium bromide staining.

2.11. Statistical analysis

Statistical significance of the data was evaluated by the Student's *t*-test. A *p*-value of 0.05 or less was considered significant.

3. Results

3.1. Preparation and stability of NPs

Six different cationic NP formulations were prepared as potential nonviral vectors. The components and the compositions of the NPs are presented in Table 1. All formulations consisted of 1 mg/ml DC-Chol as a cationic lipid. NP-T contained 5 mol% Tween 80. NP-0.3PT and NP-1PT contained 5 mol% Tween 80 with 0.3 and 1 mol% PEG_{2000}-DSPE, respectively. In the formulae of NP-0.3FT and NP-1FT for FR-targeting vectors, PEG_{2000}-DSPE in NP-0.3PT and NP-1PT was substituted with 0.3 and 1 mol% f-PEG_{2000}-DSPE, respectively. In NP-1FLT, 1 mol% f-PEG_{5000}-DSPE was used instead of f-PEG_{2000}-DSPE in NP-1FT.

The average sizes and ζ-potentials of each NP were about 100–200 nm and about +50 mV, respectively. Stability of each NP was tested by measuring the change in size with time. No significant change in the average particle size was observed in any NPs for 60 days. All formulae maintained particle size in the presence of electrostatic repulsion and/or steric hindrance of PEG lipid. These findings suggested that NPs prepared in this study were stable in water.

3.2. Characterization of nanoplexes

The physical characteristics of the nanoplexes were investigated. The charge ratio of the cationic NPs to DNA ratio was fixed at 3. The NPs were mixed with DNA and then the change in size was measured. The sizes of each nanoplex slightly increased from 200 to 300 nm (Table 2). The ζ-potential slightly decreased to +30–+40 mV. The size of nanoplex in water slightly increased by 200–350 nm after 24-h incubation (Table 2), and then did not change for up to 72 h (data not shown).

3.3. Stability of nanoplexes in the presence of serum

In serum, there are many anionic materials that would compete with and substitute for DNA in the complex. Such a substitution was assumed to be a major destabilization mechanism for the complex [25,26]. Therefore, we investigated the stability of the nanoplexes (NP-0.3FT, NP-1FT and NP-1FLT) in the presence of 10% or 50% serum. In the presence of 10% serum, the sizes of nanoplexes of NP-0.3PT and NP-1FT increased up to 500 nm, whereas that of NP-1FLT did not significantly change. In the pres-

Table 2
Particle size, stability and ζ-potential of nanoparticles and nanoplexes[a] in the absence and in the presence of serum

Formulation	Nanoparticle[b]			Nanoplex[b]			Nanoplex[c] +10% serum	Nanoplex[c] +50% serum
	Size (nm)		ζ-potential (mV)	Size (nm)		ζ-potential (mV)	Size (nm)	Size (nm)
	0 days	60 days	0 days	0 days	1 days	0 days		
NP-T	146.4	165.8	49.0	221.2	285.4	40.7	nd[d]	nd
NP-0.3PT	114.7	114.7	52.9	200.6	235.8	32.8	nd	nd
NP-1PT	139.3	127.6	53.5	191.6	214.5	40.0	nd	nd
NP-0.3FT	122.0	122.0	51.3	215.6	230.3	37.2	482.9	937.9
NP-1FT	207.4	188.3	46.8	309.1	342.9	33.3	473.0	513.0
NP-1FLT	104.3	126.3	42.3	240.5	248.2	29.6	253.4	303.5

Values represent means ($n=2$).
[a] Charge ratio (+/−) of nanoparticle/DNA=3/1.
[b] In water.
[c] 0 day after mixing of serum.
[d] Not done.

ence of 50% serum, the size of nanoplex of NP-0.3FT increased up to 900 nm, whereas that of NP-1FT and NP-1FLT slightly increased compared with that in the presence of 10% serum. Therefore, the nanoplexes of NP-1FT and NP-1FLT are more likely to maintain its physical integrity in the presence of anionic competitors.

3.4. Optimization of charge ratio in nanoplexes

In the transfection study, we focused on NP-1FT. For optimization of the charge ratio (+/−) of NPs to DNA, luciferase activity was measured in LNCaP cells transfected with NP-1FT at various charge ratios (+/−) in medium with 10% serum. The charge ratio (+/−) of 3/1 showed the highest transfection efficiency. Luciferase activity (cps/μg protein) reached about 1×10^3 at the optimal ratio (Fig. 1).

The size of NP-1FT nanoplex at the charge ratio (+/−) of 3/1 in water was not different compared with that of 1/1 and 5/1. In the presence of 10% serum, the size of NP-1FT nanoplex at the charge ratio (+/−) of 1/1, which had a −37.85 mV, increased to up to 600 nm, but those at the charge ratio (+/−) of 3/1 and 5/1, which had a positive charge, slightly increased up to about 470 nm (data not shown). In the following studies, therefore, we used a charge ratio (+/−) of 3/1 of NPs to DNA.

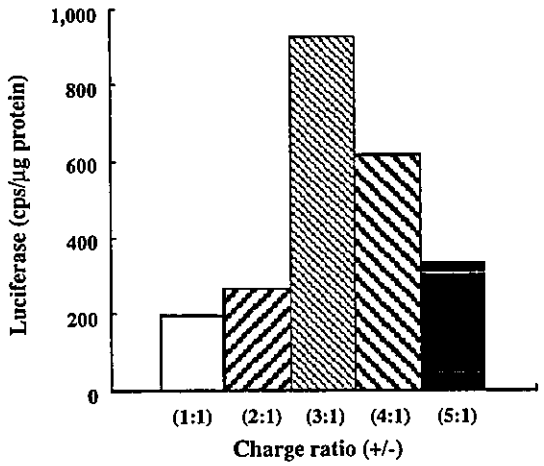

Fig. 1. Gene expressions in LNCaP cells transfected with NP-1FT at various charge ratios (+/−) in medium with 10% serum. LNCaP cells (at a density of 1×10^5 cells/well) were seeded in 6-well plates 24 h before transfection. Nanoplexes were diluted with medium with serum to a final concentration of 2 μg DNA in 1 ml medium per well, and each cell was incubated for 24 h. Each column represents the mean ($n=2$).

3.5. Association of nanoplexes with KB cells

Association of folate-linked NPs with KB cells was compared with that of nonfolate-linked NPs. We decided to use NP-T, -1FT and -1PT for comparison of the association efficiencies. The DiI, a nonexchangeable fluorescent membrane probe, labeled nanoplexes, were prepared from DiI-labeled NPs and incubated with KB cells in the presence of 10% serum. At various times, unbound nanoplexes were removed and bound nanoplexes were measured using DiI. The association of nanoplex of NP-1PT was found to be lower than that of NP-T, possibly due to addition of PEG-DSPE (Fig. 2A). However, that of NP-1FT was found to be restored 1.5-fold higher than that of NP-1PT after 3-h incubation. The presence of 1 mM free folic acid in the medium significantly reduced association with the nanoplex of NP-1FT, but not that of NP-1PT (Fig. 2B). The nanoplex of NP-1FT was taken up about 8% of the initial amount used for transfection at 3-h incubation (data not shown).

3.6. Localization of nanoplexes visualized by confocal microscopy

KB cells were exposed for 24 h to nanoplexes of DiI-labeled NP-1FT, and then fixed in 4% paraformaldehyde and visualized by confocal microscopy. The distribution pattern of DiI red signal on NP-1FT was observed throughout the cells, and the majority of the signal was concentrated in the cell surface (Fig. 3A and B). In contrast, the presence of 1 mM free folic acid in the medium reduced the signal on the cell surface (Fig. 3C and D).

As shown in Fig. 3E and F, LNCaP cells were exposed for 24 h to nanoplexes consisting of DiI-labeled NP-1FT and FITC-labeled plasmid DNA. FITC signal was detected strongly on the cell surface and weakly in cytoplasm (Fig. 3E and F). The colocalization of DiI and FITC signals was detected on the cell surface, suggesting that the plasmid DNA

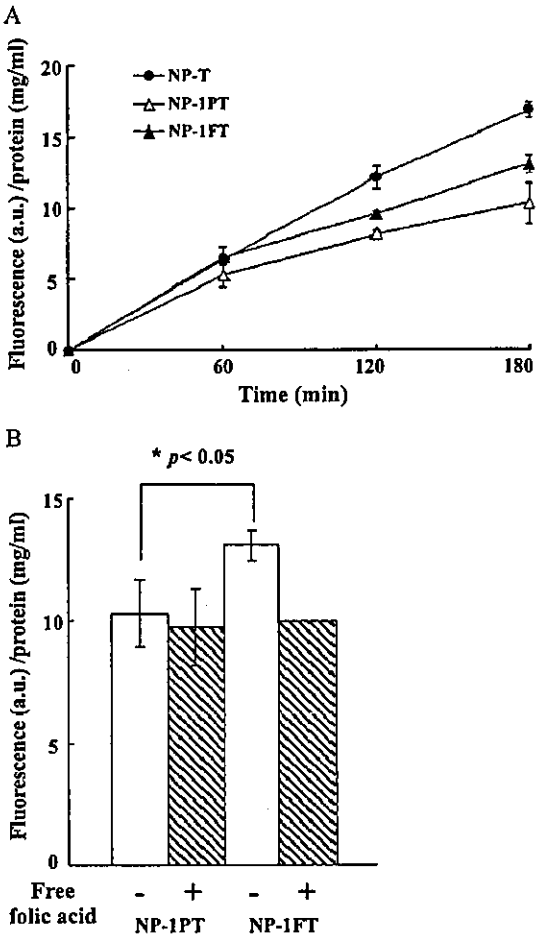

Fig. 2. Association of DiI-labeled nanoplexes with KB cells. In A, NP-T, NP-1PT or NP-1FT were mixed with 4 μg DNA at charge ratio (+/−) of 3/1. The nanoplexes were incubated with KB cells, plated overnight in a 6-well plate at 1×10^5 cells/well, in the presence of 2 ml medium containing 10% serum. After 1, 2 or 3 h, each cell was washed with PBS, detached with 0.25% trypsin from the dish and then centrifuged at 1500 × g. The pelleted cells were lysed with PBS containing 0.5% Triton X-100. Associations of DiI-labeled nanoplexes were quantified using a fluorescence plate reader at excitation and emission wavelengths of 550 and 570 nm, respectively. In B, each nanoplex was incubated with KB cells in the absence or presence of 1 mM folic acid for 3 h. Each value in A and B represents the mean ± S.D. ($n=3$). *$P<0.05$ compared with NP-1FT without free folic acid.

was still bound to NP-1FT in some places. These findings shown in Fig. 3E and F were also observed in KB cells (data not shown).

3.7. Luciferase expression in KB and LNCaP cells

We evaluated the transfection efficiency of six kinds of NPs in the presence of 10% serum by luciferase activity. KB or LNCaP cells were transfected using NPs with the plasmid coding luciferase gene for 24 h. NP-1FT showed the highest luciferase activity in the KB cells, and the other NPs showed very low luciferase activities (Fig. 4A). NP-0.3FT and -1FT showed the high luciferase activities in

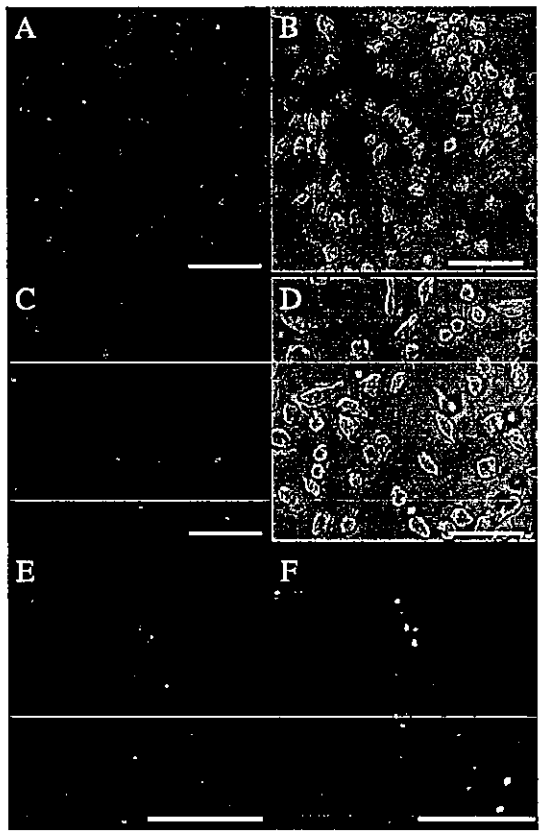

Fig. 3. Selective association of FR-targeted nanoplex with KB and LNCaP cells. KB cells were treated with the nanoplex of NP-1FT in the absence (A and B) or presence (C and D) of 1 mM folic acid for 24 h. In E and F, DiI-labeled NP-1FT was mixed with FITC-labeled DNA, and then incubated with LNCaP cells for 24 h. DiI-labeled NP-1FT and FITC-labeled DNA were visualized by confocal microscopy (magnification × 600 in panels A–D and × 1000 in panels E and F). In panels A–E, red signals show the localization of DiI-labeled NP-1FT, and in panel F, green signal shows that of FITC-labeled DNA. Scale bar = 50 μm.

LNCaP cells (Fig. 4B). Tfx20, a commercial gene transfection reagent, showed about 5-fold higher transfection efficiency in KB cells (1×10^3 cps/μg protein, equivalent with 1.9×10^3 RLU/μg protein) and about 50-fold higher in LNCaP cells (5×10^4 cps/μg protein, equivalent with 1×10^5 RLU/μg protein) than those by NP-1FT (data not shown). NP-1FLT reduced the transfection activity. In NP-0.3FT, the different profile of transfection activities was observed between both cell lines.

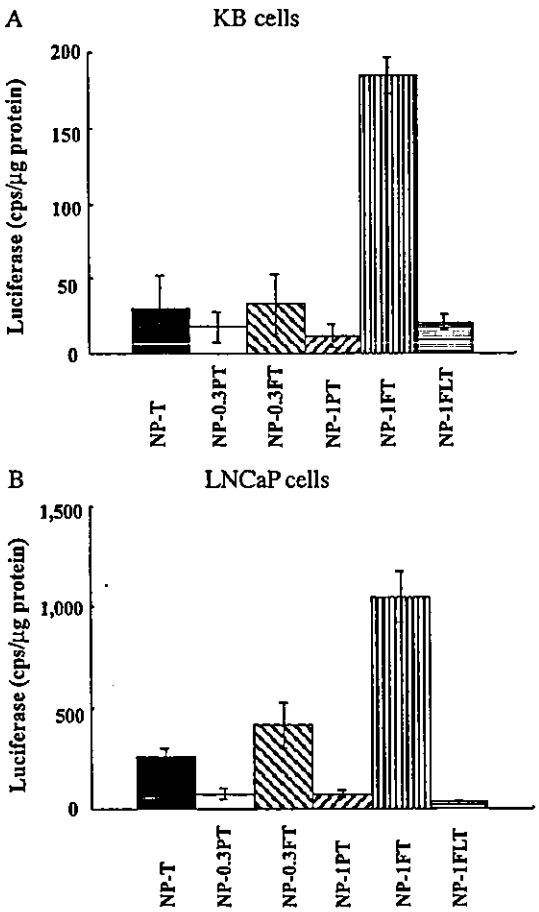

Fig. 4. Transfection into KB cells (A) and LNCaP cells (B) with FR-targeted nanoplex. Transfection particles were prepared by mixing the pCMV-Luc DNA with NPs. The cells were incubated for 24 h with transfection particles present at 2 μg DNA/ml in media with 10% serum. The cells were analyzed for luciferase activity. Each column represents the mean ± S.D. ($n=3$).

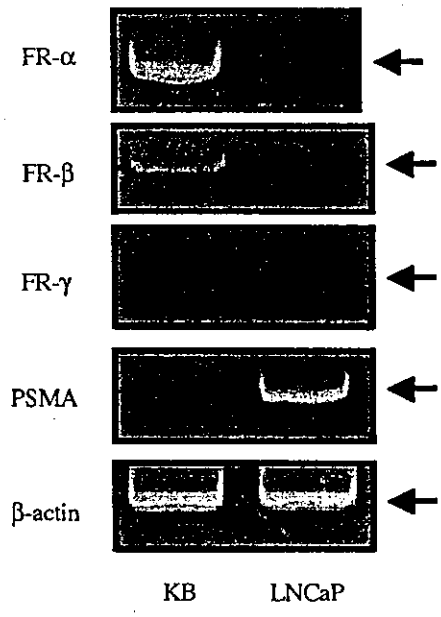

Fig. 5. FRs (FR-α, -β, -γ) and PSMA mRNA expression in KB and LNCaP cells by RT-PCR.

3.8. Expression of FRs and PSMA mRNA

Finally, to examine the mechanism of cellular uptake of folate-linked NPs, we investigated the expression of FRs in KB and LNCaP cells by RT-PCR method (Fig. 5). KB cells expressed strongly FR-α mRNA and weakly FR-β mRNA, but LNCaP cells did not. FR-γ did not express in both the cells. This suggested that FR-α and -β mediated the cellular uptake of folate-linked NPs in KB cells, but not LNCaP cells.

Therefore, it is suggested that the uptake in LNCaP cells was mediated by PSMA, and so we examined whether PSMA mRNA was expressed in LNCaP cells. PSMA mRNA was expressed strongly in LNCaP cells, but not in KB cells (Fig. 5).

4. Discussion

Although many cationic liposomes showed high gene transfer activity in vitro, their in vivo application remains limited due to their instability in serum [27]. The physical stability of the carrier and its complex

with DNA has been regarded as one of the most important factors [28]. When larger particles were administered systemically, they predominantly accumulated in the liver. This can be explained by its large mean size resulting in strong recognition of particles by the mononuclear phagocytes in the liver (Kupffer cells) [29]. A second mechanism involving the adsorption of lipoproteins on the particles cannot be ruled out. Due to the large positive ζ-potential associated with the nanoparticles, negatively charged lipoprotein present in serum would easily adsorb on its surface and accelerate the clearance from the circulation.

In preliminary experiments, we could prepare the injectable sized nanoplex using cationic NP composed of DC-Chol, f-PEG_{2000}-DSPE and PEG_{2000}-DSPE. Addition of PEG-lipid in NPs provided a stronger steric stabilization activity in the particles so that large aggregates of nanoplexes were no longer formed even in serum. However, these nanoplexes showed low transfection activity in LNCaP and KB cells (data not shown).

Recently, nonionic surfactants such as Tween 80 were used as additional additives in cationic liposomes or emulsions, presumably to enhance its physical stability [30,31]. Tween 80 may have a similar fusogenic property to DOPE and elicit its effect by stabilizing the liposomes. Therefore, addition of PEG-lipid and Tween 80 in NPs may have provided a stronger steric stabilization and fusogenic activities for the particles.

We developed cationic NPs composed of DC-Chol, Tween 80 and f-PEG-DSPE, which were given in the injectable size of about 215–300 nm (Table 2). f-PEG-DSPE and Tween 80 as a surfactant may have contributed to reduce the particle size and stabilize the nanoplex. It was reported that lipoplex is physically unstable and undergoes a change in overall structure when net charge of lipoplex approaches neutralization [3,4]. Unlike liposomes, when the ζ-potential of the nanoplexes approaches neutralization, the change in size of the nanoplexes may be minimal. Even in the presence of serum, the nanoplex did not aggregate and maintained its size (about 350 nm in NF-1FLT and about 500 nm in NP-1FT), suggesting that addition of 1 mol% PEG-DSPE and 5 mol% Tween 80 provides a stronger steric stabilization activity for the particles. This may be due to the ability of 1 mol% PEG and 5 mol% Tween 80 to shield almost completely the particle's residual positive charge.

The FR-specific delivery with DiI-labeled nanoplex of NP-1FT in KB cells was compared in the absence or presence of 1 mM folic acid in the medium. Cellular association of the nanoplex of NP-1FT with the cells was enhanced by the folate ligand (Fig. 2A) and reduced in the presence of free folic acid (Figs. 2B and 3A–D). This suggested that an association by interaction between the folate moiety of NP-1FT and FR of KB cells played a major route of transfection of nanoplex of NP-1FT.

FITC-labeled plasmid was detected strongly on the cell surface and weakly in cytoplasm (Fig. 3E and F). The colocalization of DiI and FITC signals was also detected on the cell surface, suggesting that the plasmid still bound to NP-1FT and stayed at the cell surface. Therefore, the nanoplex of NP-1FT bound to FR and then FR-mediated endocytosis may not have occurred rapidly. In addition, small amounts of PEG-lipid might prevent membrane fusion and cell internalization.

Tissue-targeted gene expression is an important issue for improvement of safety in gene therapy. Preferential expression of a gene in tumor cells contributes to the safety and the efficacy of gene therapy. The transfection efficiency of the luciferase gene was enhanced by folate-linked NPs. The highest luciferase activity in KB cells was observed in NP-1FT, and in LNCaP cells observed in NP-0.3FT and-1FT (Fig. 4), whereas low transfection activity was observed in all nonlinked NPs in both cells. NP-1FT showed slightly low transfection efficiency compared with that by Tfx20. This suggests the usefulness of NP-1FT as selective transfection reagents for the cells expressing folate binding protein. In the molecular weight of PEG, f-PEG_{2000}-DSPE will be suitable for high transfection with selectivity since f-PEG_{5000}-DSPE may reduce the cell association through steric hindrance. However, it is not clear why the different patterns of transfection activity in NP-0.3FT between the two kinds of cell lines were observed. The distribution density of folate binding protein on the cell surface in LNCaP cells might be higher than that in KB cells.

Finally, we investigated the expression of FRs in KB and LNCaP cells. There are three folate receptor isoforms, α, β and γ, with distinctive patterns of tissue distribution. FR-α is predominantly expressed

in most normal and malignant epithelial tissues [13,14], FR-β in some nonepithelial malignancies [16, 17] and FR-γ in hematopoietic cells [18,19]. FR-α and FR-β mRNA were expressed in KB cells (Fig. 5). The uptake of NPs in KB cells may be mediated via FR-α and-β.

PSMA is homologous to the transferrin receptor with an overexpression pattern restricted to prostate cancer cells and malignant human prostate tissue and is known to have the ability to remove the glutamate residues from folate-poly-γ-glutamate [23]. It was reported that human prostate contains folate-binding proteins [21], and that folic acid binds to the membrane fraction that cross-reacts with anti-PSMA antibody [23]. It is suggested that uptake of folate-linked NPs in LNCaP cells might be mediated by PSMA, and therefore we examined the expression of PSMA mRNA. In LNCaP cells, PSMA mRNA was abundantly expressed, but FR mRNAs were not (Fig. 5). This suggested that the folate-linked NPs bound to PSMA and then were taken up by LNCaP cells. This study is the first to report that folate-linked NPs can selectively deliver DNA to prostate cancer and then enhance the gene expression.

5. Conclusions

We have shown that NPs based on the DC-Chol, f-PEG_{2000}-DSPE and Tween 80 could form injectable nanoplexes with high transfection of the luciferase gene in human oral cancer and prostate cancer cells. Such folate-linked nanoparticles are potentially useful as prostate tumor-specific vectors for gene therapy. Further studies on in vivo gene delivery are now underway to evaluate the efficacy and safety of the present system.

Acknowledgements

We thank Mr. Tomonori Shiokawa and Mr. Masayoshi Fukushima for assistance in the experimental work. We also thank Dr. Kazuhiro Kubo (NOF, Tokyo, Japan) for supplying PEG-DSPE.

This project was supported in part by a grant from the Promotion and Mutual Aid Corporation for Private Schools of Japan and by a Grant-in-Aid for Scientific Research from the Ministry of Education, Culture, Sports, Science, and Technology of Japan.

References

[1] C.R. Dass, M.A. Burton, Lipoplexes and tumours. A review, J. Pharm. Pharmacol. 51 (1999) 755–770.
[2] D.A. Treco, R.F. Selden, Non-viral gene therapy, Mol. Med. Today 1 (1995) 314–321.
[3] B. Sternberg, F.L. Sorgi, L. Huang, New structures in complex formation between DNA and cationic liposomes visualized by freeze-fracture electron microscopy, FEBS Lett. 356 (1994) 361–366.
[4] E. Lai, J.H. van Zanten, Real time monitoring of lipoplex molar mass, size and density, J. Control. Release 82 (2002) 149–158.
[5] N.K. Egilmez, Y. Iwanuma, R.B. Bankert, Evaluation and optimization of different cationic liposome formulations for in vivo gene transfer, Biochem. Biophys. Res. Commun. 221 (1996) 169–173.
[6] M. Nishikawa, L. Huang, Nonviral vectors in the new millennium: delivery barriers in gene transfer, Hum. Gene Ther. 12 (2001) 861–870.
[7] J.A. Reddy, D. Dean, M.D. Kennedy, P.S. Low, Optimization of folate-conjugated liposomal vectors for folate receptor-mediated gene therapy, J. Pharm. Sci. 88 (1999) 1112–1118.
[8] M.A. Gosselin, R.J. Lee, Folate receptor-targeted liposomes as vectors for therapeutic agents, Biotechnol. Annu. Rev. 8 (2002) 103–131.
[9] J.A. Reddy, C. Abburi, H. Hofland, S.J. Howard, I. Vlahov, P. Wils, C.P. Leamon, Folate-targeted, cationic liposome-mediated gene transfer into disseminated peritoneal tumors, Gene Ther. 9 (2002) 1542–1550.
[10] H.E. Hofland, C. Masson, S. Iginla, I. Osetinsky, J.A. Reddy, C.P. Leamon, D. Scherman, M. Bessodes, P. Wils, Folate-targeted gene transfer in vivo, Mol. Ther. 5 (2002) 739–744.
[11] J. Sudimack, R.J. Lee, Targeted drug delivery via the folate receptor, Adv. Drug Deliv. Rev. 41 (2000) 147–162.
[12] S. Ni, S.M. Stephenson, R.J. Lee, Folate receptor targeted delivery of liposomal daunorubicin into tumor cells, Anticancer Res. 22 (2002) 2131–2135.
[13] P.C. Elwood, Molecular cloning and characterization of the human folate-binding protein cDNA from placenta and malignant tissue culture (KB) cells, J. Biol. Chem. 264 (1989) 14893–14901.
[14] M. Wu, W. Gunning, M. Ratnam, Expression of folate receptor type alpha in relation to cell type, malignancy, and differentiation in ovary, uterus, and cervix, Cancer Epidemiol. Biomark. Prev. 8 (1999) 775–782.
[15] F. Shen, J.F. Ross, X. Wang, M. Ratnam, Identification of a novel folate receptor, a truncated receptor, and receptor type beta in hematopoietic cells: cDNA cloning, expression, immunoreactivity, and tissue specificity, Biochemistry 33 (1994) 1209–1215.
[16] M. Ratnam, H. Marquardt, J.L. Duhring, J.H. Freisheim, Ho-

mologous membrane folate binding proteins in human placenta: cloning and sequence of a cDNA, Biochemistry 28 (1989) 8249–8254.
[17] J.F. Ross, H. Wang, F.G. Behm, P. Mathew, M. Wu, R. Booth, M. Ratnam, Folate receptor type beta is a neutrophilic lineage marker and is differentially expressed in myeloid leukemia, Cancer 85 (1999) 348–357.
[18] H. Wang, J.F. Ross, M. Ratnam, Structure and regulation of a polymorphic gene encoding folate receptor type gamma/gamma', Nucleic Acids Res. 26 (1998) 2132–2142.
[19] X. Wang, G. Jansen, J. Fan, W.J. Kohler, J.F. Ross, J. Schornagel, M. Ratnam, Variant GPI structure in relation to membrane-associated functions of a murine folate receptor, Biochemistry 35 (1996) 16305–16312.
[20] X. Gao, A.T. Porter, D.J. Grignon, J.E. Pontes, K.V. Honn, Diagnostic and prognostic markers for human prostate cancer, Prostate 31 (1997) 264–281.
[21] J. Holm, S.I. Hansen, M. Hoier-Madsen, High-affinity folate binding in human prostate, Biosci. Rep. 13 (1993) 99–105.
[22] D.A. Silver, I. Pellicer, W.R. Fair, W.D. Heston, C. Cordon-Cardo, Prostate-specific membrane antigen expression in normal and malignant human tissues, Clin. Cancer Res. 3 (1997) 81–85.
[23] J.T. Pinto, B.P. Suffoletto, T.M. Berzin, C.H. Qiao, S. Lin, W.P. Tong, F. May, B. Mukherjee, W.D. Heston, Prostate-specific membrane antigen: a novel folate hydrolase in human prostatic carcinoma cells, Clin. Cancer Res. 2 (1996) 1445–1451.
[24] A. Gabizon, A.T. Horowitz, D. Goren, D. Tzemach, F. Mandelbaum-Shavit, M.M. Qazen, S. Zalipsky, Targeting folate receptor with folate linked to extremities of poly(ethylene glycol)-grafted liposomes: in vitro studies, Bioconjug. Chem. 10 (1999) 289–298.
[25] J. Zabner, Cationic lipids used in gene transfer, Adv. Drug Deliv. Rev. 27 (1997) 17–28.
[26] V. Escriou, C. Ciolina, F. Lacroix, G. Byk, D. Scherman, P. Wils, Cationic lipid-mediated gene transfer: effect of serum on cellular uptake and intracellular fate of lipopolyamine/DNA complexes, Biochim. Biophys. Acta 1368 (1998) 276–288.
[27] D.L. Reimer, S. Kong, M. Monck, J. Wyles, P. Tam, E.K. Wasan, M.B. Bally, Liposomal lipid and plasmid DNA delivery to B16/BL6 tumors after intraperitoneal administration of cationic liposome DNA aggregates, J. Pharmacol. Exp. Ther. 289 (1999) 807–815.
[28] O. Zelphati, C. Nguyen, M. Ferrari, J. Felgner, Y. Tsai, P.L. Felgner, Stable and monodisperse lipoplex formulations for gene delivery, Gene Ther. 5 (1998) 1272–1282.
[29] T. Sakaeda, K. Hirano, Effect of composition on biological fate of oil particles after intravenous injection of O/W lipid emulsions, J. Drug Target. 6 (1998) 273–284.
[30] F. Liu, J. Yang, L. Huang, D. Liu, Effect of non-ionic surfactants on the formation of DNA/emulsion complexes and emulsion-mediated gene transfer, Pharm. Res. 13 (1996) 1642–1646.
[31] T.W. Kim, H. Chung, I.C. Kwon, H.C. Sung, S.Y. Jeong, Optimization of lipid composition in cationic emulsion as in vitro and in vivo transfection agents, Pharm. Res. 18 (2001) 54–60.

5

機能性脂質マイクロエマルションとDDS

米谷 芳枝*
Maitani Yoshie

Summary

機能性脂質マイクロエマルションとして，注射用血中滞留性マイクロエマルション，葉酸修飾マイクロエマルション，トリプシン修飾遺伝子ベクター，鼻腔投与用キトサン被覆マイクロエマルションを調製し，癌化学療法，癌遺伝子治療，粘膜ワクチンに応用した。血中滞留性マイクロエマルションは，マイクロエマルションをポリエチレングリコール（PEG）脂質で修飾して調製し，アクラルビシン，ビンクリスチン，パクリタキセルを封入した。葉酸修飾マイクロエマルションは，血中滞留性マイクロエマルションのPEG脂質の先端の一部を葉酸で修飾し，癌組織に高発現している葉酸受容体に，抗癌薬をターゲティングする，癌ターゲティング治療を目指した。トリプシン修飾マイクロエマルション遺伝子ベクターでは，癌細胞周辺の組織を破壊して，癌細胞にまで遺伝子を運べるように，エマルションの表面をトリプシンで修飾した。キトサン被覆マイクロエマルションワクチン製剤は，正電荷で鼻粘膜に付着し，抗原提示細胞に取り込まれ，IgA（イムノグロブリンA）を産生した。

1．はじめに

微粒子製剤は，薬物を標的部位に集積させて，副作用を軽減し，薬効を高めることができるので，DDS（drug delivery system；薬物送達システム）において注目されている。薬物の微粒子担体には，マイクロスフェア，マイクロカプセル，リポソーム，エマルション，高分子ミセルなどがある。エマルションにおいて，界面活性剤としてリン脂質を使ったものを，特に，脂肪乳剤という。私達のマイクロエマルションの特徴は，ナノサイズのエマルションを簡単な調製法で，表面修飾して機能性マイクロエマルションにしている点である。機能性脂質マイクロエマルションには，PEG（polythylene glycol）脂質で修飾した血中滞留性エマルションや，癌ターゲティング用葉酸修飾マイクロエマルションやトリプシン修飾遺伝子ベクターがある。（図1）。ここでは，機能性マイクロエマルション製剤による，癌化学療法，遺伝子治療，免疫治療への応用について紹介する。

2．マイクロエマルション

一般には，エマルションは，水に油と乳化剤を加えて機械的に乳化して調製される。その粒子サイズは，約0.2～10 μm のものが多い。マイクロエマルションの定義は，元来は，瞬時に調製され，

*星薬科大学医薬品化学研究所創剤構築研究室・教授

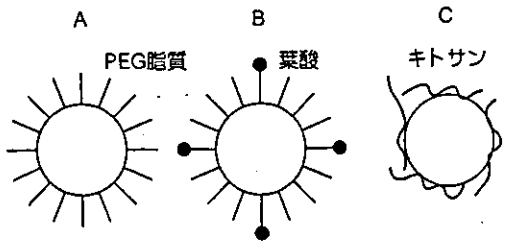

図1 血中滞留性マイクロエマルション（A），葉酸修飾マイクロエマルション（B），キトサン被覆マイクロエマルション（C）
PEG脂質で表面修飾したマイクロエマルション（A），PEG脂質の先端の一部を葉酸で修飾した癌ターゲティング用マイクロエマルション（B），正電荷マイクロエマルション（C）．
PEG：polyethylene glycol

透明で安定なエマルションという意味で，小さなサイズの油滴という意味ではないが，現在，両方の意味で広義に用いられている。

エマルションの利点は，脂肪乳剤に代表されるように，製剤としての安全性や安定性が高いこと，また，多くの薬物で見られる，難水溶性の薬物を溶解できること，などである。欠点は，親水性薬物は封入できないこと，などである。これまでに，点滴注射用脂肪乳剤や経口投与製剤が市販されている。経口投与製剤では，シクロスポリンMEPC(micro-emulsion pre-concentrate，前濃縮物製剤)（ネオーラル® ）が商品化されている[1]。これは，自己乳化システム（self-emulsifying drug delivery systems，SEDDS）で，薬物と油と界面活性剤溶液を，ゼラチンカプセルに詰めたもので，飲んだ水でエネルギーを加えることなく，腸管内で瞬時にマイクロエマルションを形成する。

私達のマイクロエマルションも同じように，脂質をエタノールに溶解し，濃縮後，水を添加すると瞬時に形成される。（図2）。この方法で，ナノサイズの微粒子を，超音波などのような外部からのエネルギーや，有害な有機溶媒を用いず，短時間に調製できる[2]。

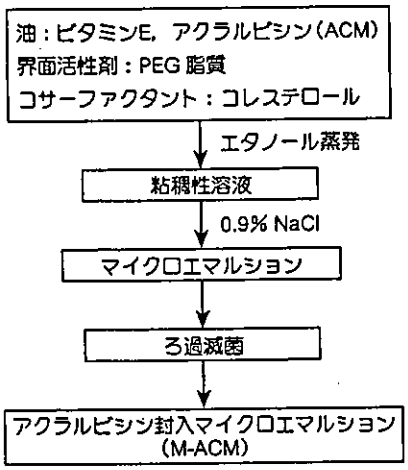

図2 注射用マイクロエマルション調製法
ビタミンEの油にACMを溶かし，これとPEG脂質，コレステロールをエタノールに溶解後，エタノールを蒸発させ，水を加えると，直ちにマイクロエマルションが形成される。

3．注射用抗癌剤封入血中滞留性マイクロエマルション製剤

一般に，微粒子は，静脈内投与すると，血液成分との相互作用ののち，単核食細胞系に認識され，体循環血から除去される。そこで，血中滞留性エマルションでは，血液成分を吸着しにくくするために，PEGで修飾した。腫瘍部位では，血管壁がうすく，薬液が漏れやすくなっているので，血中滞留性リポソームは，抗癌剤の腫瘍部位への集積（受動的ターゲティング）が可能となる。既に，ドキソルビシン血中滞留性リポソーム製剤（Doxil® ）が，欧米では発売されている。しかし，血中滞留性エマルションは，研究報告もまだ極めて少ない。血中滞留性エマルションでは，リポソームに封入しにくい疎水性薬物の，腫瘍部位への受動的ターゲティングが可能となる。

塩酸アクラルビシン(アクラシノン，ACM)，硫酸ビンクリスチン(オンコビン，VCR)，パクリタキセル（タキソール® ）は，疎水性薬物で，リポソームに封入しにくく，水溶液中で不安定である。そこで，界面活性剤とコサーファクタントとして，コレステロールとPEG脂質からなる，アク

ラルビシン封入血中滞留性エマルション（M-ACM）[3]，ビンクリスチン封入血中滞留性マイクロエマルション（M-VCR）[4]，パクリタキセル（Paclitaxel）封入血中滞留性マイクロエマルション（M-Paclitaxel）[5]を開発した。PEG脂質は，血中滞留性の機能だけでなく，両親媒性で良い乳化剤となるので，マイクロエマルションを調製しやすい[6]。M-ACMやM-VCRの平均粒子サイズは140nm以下で，薬物封入率は95%以上であった。また，遮光下7℃で1年間の保存では，製剤として安定であった。

M-ACMでは，マウスにおいて，ACMの血中滞留性が高くなり，固形癌に対する抗腫瘍効果も，フリーのACMに比べて投与量に応じて高くなった。M-VCRもマウスにおいて血中滞留性を示し，VCRが腫瘍に蓄積して，固形癌に対する抗腫瘍効果もフリーの薬物に比べて高くなった[4]。（図3，表1）。

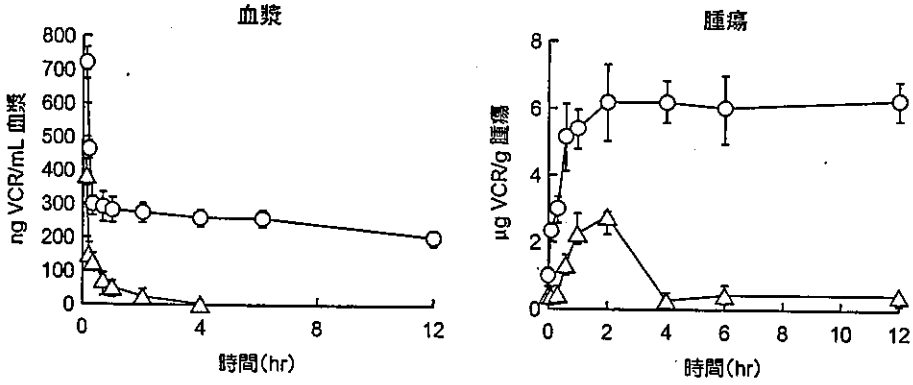

図3　ビンクリスチン封入マイクロエマルション（M-VCR）の体内動態
○：M-VCR，△：フリーVCR（ビンクリスチン生理食塩水〔0.1mg/mL〕）
ビンクリスチン封入マイクロエマルションを2mg/kgマウスでM5076固形癌のマウスに静脈内投与したときの血中濃度と腫瘍内薬物濃度の時間変化．
マイクロエマルションでは，薬物は注射12時間後でも血中に検出され，固形癌に集積した．
（文献4より）

表1　ビンクリスチン封入マイクロエマルション（M-VCR）の抗腫瘍効果
VCR封入マイクロエマルションの固形癌に対する抗腫瘍効果は，フリーの薬物に比べて高くなった．

製剤	投与量 (mg VCR/kg)	腫瘍重量 (g ± SD)	腫瘍重量減少率 (%)	
生理食塩液	コントロール	1.2 ± 0.2	---	
M（薬物不含）	コントロール	1.2 ± 0.3	0	
フリーVCR	1.25	0.7 ± 0.2	42	]*
M-VCR	1.25	0.4 ± 0.2	67	]*

腫瘍を移植後，5日目に5日ごとに4回繰り返し静脈内投与．
＊：$p < 0.01$
M：薬物封入マイクロエマルション
フリーVCR：ビンクリスチン生理食塩水（0.1mg/mL）
M-VCR：ビンクリスチン封入マイクロエマルション
（文献4より）

M-Paclitaxelでは，難溶性である薬物を，界面活性剤とコサーファクタントとして，PEG脂質やコレステロール，Tween80と大豆油を用いて，薬物封入率の高いマイクロエマルション製剤とした。M-Paclitaxelの薬物分布の模式図を，図4に示す。薬物は，油滴の内部と表面に，分布していると考えられる。人工ニュラルネットワークを用いて，各成分の製剤に対する寄与を解析すると，PEG脂質は薬物封入率と粒子サイズに，Tween80は製剤の安定性に，それぞれ関与していることが明らかになった[5]。

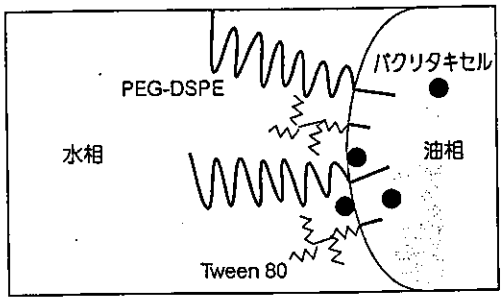

図4 パクリタキセル封入マイクロエマルション(o/w)の薬物分布の模式図
マイクロエマルションの平均粒子径は262nmで，薬物を96.7%含有した．薬物は，油滴の内部と表面に分布し，PEG脂質が薬物封入率と粒子サイズに，Tween80が製剤の安定性にそれぞれ関与している．
o/w：oil in water
PEG-DSPE：polyethylene glycol-distearoylphosphatidyl ethanolamine

4．注射用アクラルビシン封入葉酸修飾マイクロエマルション製剤

葉酸受容体は，卵巣，乳房，結腸，肺の上皮癌などにおいて，過剰発現していることが知られているので，葉酸をリガンドとした担体は，癌細胞にターゲティングが可能となる。従って，アクラルビシン封入葉酸修飾マイクロエマルション(FM-ACM)は，PEG修飾によって血中滞留したM-ACMに，さらに一部のPEG鎖の先端を，葉酸によって修飾したものである。FM-ACMは，葉酸脂質あるいは，葉酸-PEG脂質(PEG分子量2,000，5,000)(図5)，PEG脂質(分子量2,000)，コレステロール，ビタミンEを含有する。

葉酸修飾による細胞内への，ターゲティング能を評価するため，蛍光ラベル物質である1,1'-

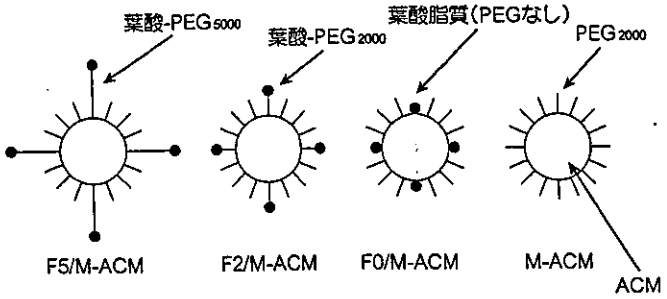

図5 アクラルビシン(ACM)封入葉酸修飾マイクロエマルション
マイクロエマルションは，葉酸-PEG脂質：PEG脂質：コレステロール：ビタミンE：ACM＝0.24：6.7：48.3：43.3：1.5(mol%)で，平均粒子径は約120nm，ACM封入率約80%である．
PEG：polyethylene glycol. PEGの後ろにある数値は，分子量．
F5/M-ACM：葉酸-PEG脂質(5,000)で修飾したM-ACM
F2/M-ACM：葉酸-PEG脂質(2,000)で修飾したM-ACM
F0/M-ACM：葉酸脂質で修飾したM-ACM
M-ACM：封入マイクロエマルション(PEG脂質2,000からなるエマルション)
ACM：アクラルビシン (文献7より)

Dioctadecyl-3,3,3',3'-tetramethylindocarbocyanine perchlorate (DiI) でラベルした，葉酸修飾マイクロエマルションの，ヒト咽頭上皮癌細胞（KB細胞）への取り込み量を測定した結果，葉酸修飾によって，取り込みは高くなった。また，フリーの葉酸により，取り込みが阻害されることから，競合阻害が起きていると考えられ，細胞内への取り込みは，葉酸受容体を介していることが確認された。また，葉酸修飾PEG脂質のPEG鎖の長さによる，葉酸受容体の認識能への影響を，*in vitro* 抗癌作用から調べた結果，PEG脂質のPEG鎖が，分子量5,000(F5/M-ACM)のとき，2,000(F2/M-ACM)のときよりも，細胞内へのACMの取り込みが高くなった。(図6)。担癌マウスにおける抗

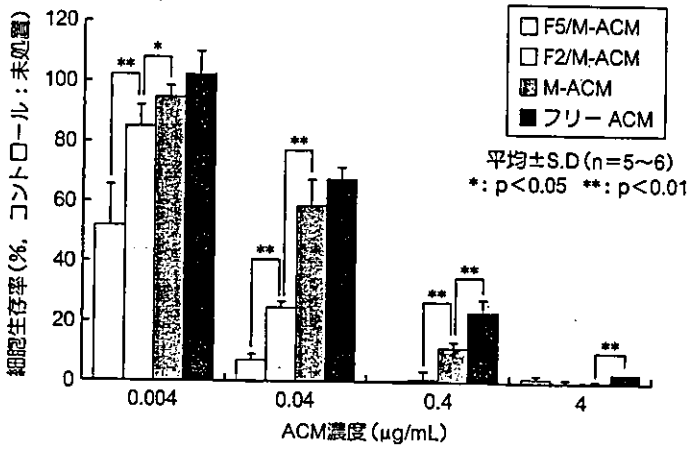

図6　アクラルビシン封入葉酸修飾マイクロエマルションの *in vitro* 抗腫瘍効果

PEG鎖5,000に葉酸修飾したマイクロエマルションF5/M-ACMは，細胞生存率を低下し，高い抗腫瘍効果を示した．この効果はフローサイトメトリーによる細胞への取り込み量と相関するものであった．

PEG：polyethylene glycol
F5/M-ACM：葉酸-PEG脂質(5,000)で修飾したM-ACM
F2/M-ACM：葉酸-PEG脂質(2,000)で修飾したM-ACM
M-ACM：封入マイクロエマルション(PEG脂質2,000からなるエマルション)
フリーACM：ACM生理食塩水

(文献7より)

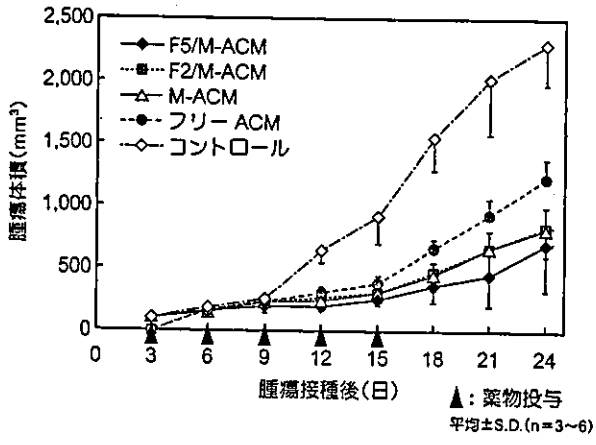

図7　アクラルビシン封入葉酸修飾マイクロエマルション静脈内投与による抗腫瘍効果

F5/M-ACMは最も高い抗腫瘍効果を示した．葉酸修飾マイクロエマルションは *in vivo* においても有用であることが確認された．

F5/M-ACM：葉酸-PEG脂質(5,000)で修飾したM-ACM
F2/M-ACM：葉酸-PEG脂質(2,000)で修飾したM-ACM
M-ACM：封入マイクロエマルション(PEG脂質2,000からなるエマルション)
フリーACM：ACM生理食塩水
control：生理食塩水　(文献7より)

腫瘍効果より，マイクロエマルション製剤を葉酸で修飾することにより，ACMの高い抗癌作用が得られた。特に，葉酸修飾PEG鎖が分子量5,000のとき，ターゲティング能が高くなることが明らかになった[7]。(図7)。

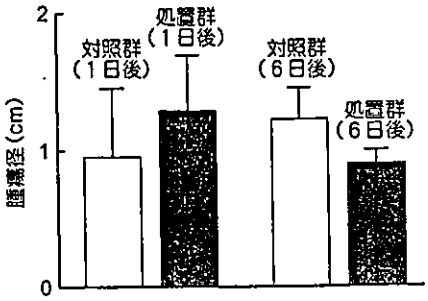

図8 ミドカインプロモータ自殺遺伝子とトリプシン修飾血中滞留性マイクロエマルションベクターによる自殺遺伝子治療における抗腫瘍効果

ヒト膵臓固形癌のサイズが約1 cmになったとき，ベクター/遺伝子の荷電比=4/1で自殺遺伝子とガンシクロビルを10 μg/腫瘍で2日間ごとに2回腫瘍内注射した．(平均±SD，n=3)

遺伝子導入の結果，腫瘍の縮小が観察された．

(文献8より)

5．トリプシン修飾マイクロエマルション遺伝子ベクター

外来遺伝子の導入による癌治療の1つに，プロドラッグ療法の自殺遺伝子治療がある。これは，腫瘍部位に導入した，単純ヘルペスウイルスチミジンキナーゼ(HSV-tk)がチミジンキナーゼ(tk)を発現させ，この酵素によって，プロドラッグが活性代謝物になって，癌細胞を死滅させるものである。腫瘍細胞特異的に，治療遺伝子を発現させて，腫瘍の治療を行うために，腫瘍細胞特異的に，遺伝子を運搬する微粒子と，腫瘍細胞内で，導入遺伝子を，特異的に発現させるプロモータを選択した。ミドカインは，消化器系癌や神経芽腫など，色々な癌の進行癌に，高頻度に発現している。従って，癌ターゲティングのために，ミドカインプロモータのtk遺伝子を用いた。微粒子担体としては，トリプシン修飾して，癌細胞周辺の組織を破壊して，癌細胞にまで遺伝子を運べるように，トリプシン修飾血中滞留性マイクロエマルションベクターをデザインした。これは，油相としてビタミンE，また界面活性剤とコサーファクタントとして，DC-コレステロール，コレステ

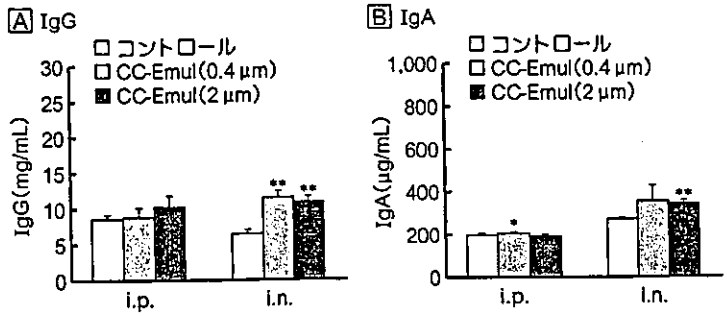

図9 オブアルブミンとコレラトキシンを吸着させた粒子径約0.4 μmと2 μmのキトサン被覆エマルション(CC-Emul)をラット腹腔内と鼻腔投与したときのIgG(A)とIgA(B)

投与は0，14，28日目にして，35日目に採血した．平均値±S.D(n=3～5)．＊：$p<0.05$，＊＊：$p<0.01$ コントロールと比較．コントロールはオブアルブミン(5 mg/kg)とコレラトキシン(2.5mg/kg)のみ．粒子径約2 mmのCC-Emulの鼻腔内投与は，腹腔内投与より高く，コントロールに対して有意に高いIgGとIgAを産生した．

(文献9より)